Electronic Supplementary Material (ESI) for Journal of Materials Chemistry C
This journal is © The Royal Society of Chemistry 2013

J. Mat. Chem. C

Dynamic Article Links ►

Cite this: DOI: 10.1039/c0xx00000x

www.rsc.org/xxxxxx

Supporting Information

Intramolecular Redox-Induced Dimerization in a Viologen Dendrimer

Kuldeep Wadhwa[a] Selbi Nuryyeva,[a] Albert C. Fahrenbach,[b] Mourad Elhabiri,*[c] Carlos Platas-Iglesias,*[d] and Ali Trabolsi*[a]

[a]*New York University Abu Dhabi, Center for Science and Engineering, Abu Dhabi, United Arab Emirates*
[b]*Department of Chemistry, Northwestern University, 2145 Sheridan Road, Evanston, Illinois 60208, United States*
[c]*Laboratoire de Chimie Bioorganique et Médicinale, UMR 7509 CNRS-Université de Strasbourg, ECPM, 25 rue Becquerel, 67200 Strasbourg, France*
[d]*Departamento de Química Fundamental, Universidade da Coruña, Campus da Zapateira-Rúa da Fraga 10, 15008 A Coruña, Spain.*
*E-mail:ali.trabolsi@nyu.edu

Supporting Information

* Correspondence Address		
Professor Ali Trabolsi *Center for Science and Engineering* New York University Abu Dhabi Abu Dhabi, UAE Tel: (+971)-26284575 Fax: (+971)-26238616 E-Mail: ali.trabolsi@nyu.edu	**Dr Mourad Elhabiri** *Laboratoire de Chimie Bioorganique et Médicinale*, UMR 7509 CNRS-Université de Strasbourg, ECPM, 25 rue Becquerel, 67200 Strasbourg, France	**Dr Carlos Platas-Iglesias** *Departamento de Química Fundamental*, Universidade da Coruña, Campus da Zapateira-Rúa da Fraga 10, 15008 A Coruña, Spain

** The research described here was sponsored by New York University Abu Dhabi, in Abu Dhabi in the UAE. K. W., S. G. N., and A. T. thank NYUAD for their generous support of this program of research at NYUAD. A. C. F. thanks the National Science Foundation (NSF) for the award of a NSF Graduate Research Fellowship. M.E. thanks the Centre National de la Recherche Scientifique and the University of Strasbourg (UMR 7509 CNRS-UdS) in France for financial support. C. P.-I. thanks Centro de Supercomputación de Galicia (CESGA) for providing the computer facilities.

1. General Methods:

All reagents were purchased from commercial suppliers (Aldrich) and used without further purification. Thin layer chromatography was used to follow the reactions and was performed on silica gel 60 F254 (E. Merck). Routine Nuclear Magnetic Resonance (NMR) spectra were recorded at 298 K on a Bruker Advance 600 spectrometer with a working frequency of 600 and 150 MHz for ^{1}H and ^{13}C, respectively. Chemical shifts are reported in ppm relative to the signal corresponding to the residual non-deuterated solvent ($CDCl_3$ ($\delta = 7.26$), CD_3CN ($\delta = 1.94$), D_2O ($\delta = 4.97$), and DMSO-d_6 ($\delta = 2.50$). Zinc dust was activated by stirring it with dilute HCl during 10–15 minutes, and then washing several times with distilled H_2O, EtOH and absolute Et_2O before drying rigorously. This procedure removes oxides, which form slowly upon standing in air from the surface of zinc.[1] All the physicochemical investigations were carried out with spectroscopic grade acetonitrile (MeCN, Sigma Aldrich ≥ 99.9% for spectroscopy). The stock solutions of **HV**•12PF_6 and **BMV**•2PF_6 were prepared by weighing using a Sartorius analytical balance (precision 0.1 mg). Complete dissolution of **HV**$^{12+}$ and **BMV**$^{2+}$ was achieved using an ultrasonic bath (Branson 2510). The concentrations were thus obtained by weighing the appropriate amounts. Reduction of **HV**$^{12+}$ and **BMV**$^{2+}$ into the corresponding radical cations was achieved under argon (CO_2- and O_2-free argon) in less than 1 h by vigorous stirring with activated zinc dust in argon-purged MeCN. The formation of the radicals was monitored by absorption spectrophotometry using Cary 5000 UV-Vis-NIR spectrophotometer. High-resolution mass spectra were measured on an Agilent 6540 UHD Accurate-Mass Q-TOF LC/MS spectrometer (HR-ESI). Cyclic voltammetry (CV) was carried out at room temperature in argon-purged DMF solutions with a Gamry Multipurpose instrument (Reference 600) interfaced to a PC. The CV experiments were performed using a glassy carbon working electrode (0.071 cm^2, BASi). The electrode surface was polished routinely with 0.05 μm alumina-water slurry on a felt surface immediately before use. The counter electrode was a Pt coil and the reference electrode was a Ag/AgCl electrode, unless otherwise noted. The concentration of samples were 1.0×10^{-3} M and 0.17×10^{-3} M for **BMV**$^{2+}$ and **HV**$^{12+}$, respectively. The concentration of the supporting electrolyte, tetrabutylammonium hexafluorophosphate ($TBAPF_6$), was 0.1 M in all experiments. Experimental errors: potential values, ± 10 mV for cyclic voltammetry and ± 1 mV for square wave differential pulse. Digital simulations of the CV data (dimerization constants) were performed using DigiSim. ITO coated glass slides (reference ITO-48-R10), 4-8 Ohms were purchased and used as they are from Cytodiagnostics.

2. Synthetic strategy employed in the preparation of hexakis(4-chloromethylphenoxy)cyclotriphosphazene (5)

The synthesis of the hexaviologen-phosphorus dendrimer (**HV^{12+}**) was achieved in 82% yield (Scheme 1a) following the reaction of the hexachlorodendrimer (**3**) with 1-methyl-4,4'-bipyridinium (noted monomethylbipyridinium **MB**$^{+}$) in MeCN. **HV**•$12PF_6$ was obtained in quantitative yield from the water soluble intermediate **HV**•6I•6Cl after counter ion exchange with a saturated solution of tetrabutylammonium hexafluorophosphate ($TBAPF_6$) in H_2O. The hexafunctional core, namely hexachlorocyclotriphosphazene ($N_3P_3Cl_6$), was first functionalized on its P atoms with *p*-hydroxybenzaldehyde groups . The aldehyde groups were further reduced to alcohol before the conversion to the more reactive benzyl chloride moieties following the procedure reported in the literature.[2]

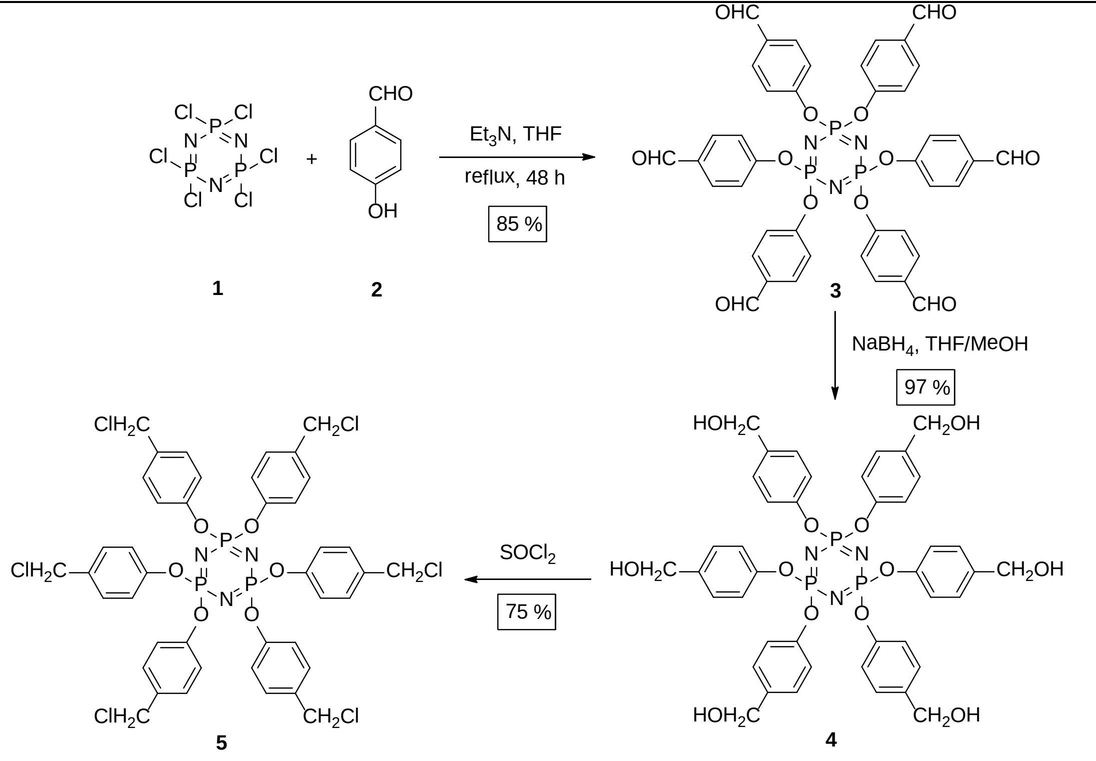

Scheme S1: Synthetic route for the synthesis of hexakis(4-chloromethylphenoxy)cyclotriphosphazene (**5**)

3. Synthesis of hexakis(4-formylphenoxy)cyclotriphosphazene (3)

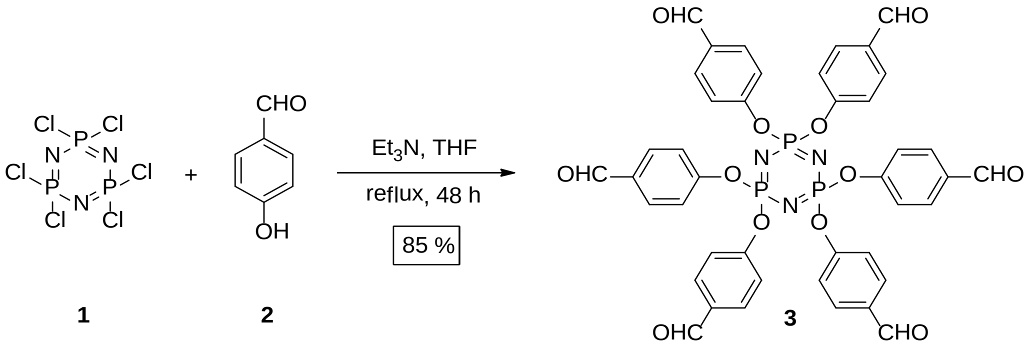

Compound **3** was prepared according to the literature[2] with some modifications. To a solution of **1** (10.2 g, 0.03 mol) in 50 mL THF was added a solution of *p*-hydroxybenzaldehyde **2** (23.0 g, 0.19 mol) and triethylamine (24.1 g, 0.24 mol). The reaction mixture was refluxed for 24 h. After filtration the solvent was removed under reduced pressure. The residue was recrystallized from ethylacetate to afford **3** as white solid. Yield: 85 %. ^{1}H NMR (600 MHz, $CDCl_3$) δ: 9.96 (s, 6H), 7.76 (d, *J* = 8.4 Hz, 12 H), 7.11 (d, *J* = 7.2 Hz, 12 H); ^{13}C NMR (600 MHz, $CDCl_3$) *δ*: 190.4, 154.5, 133.8, 131.4, 121.2 ppm; ^{31}P NMR (600 MHz, $CDCl_3$) *δ*: 7.07 ppm.

4. Synthesis of hexakis(4-hydroxymethylphenoxy)cyclotriphosphazene (4)

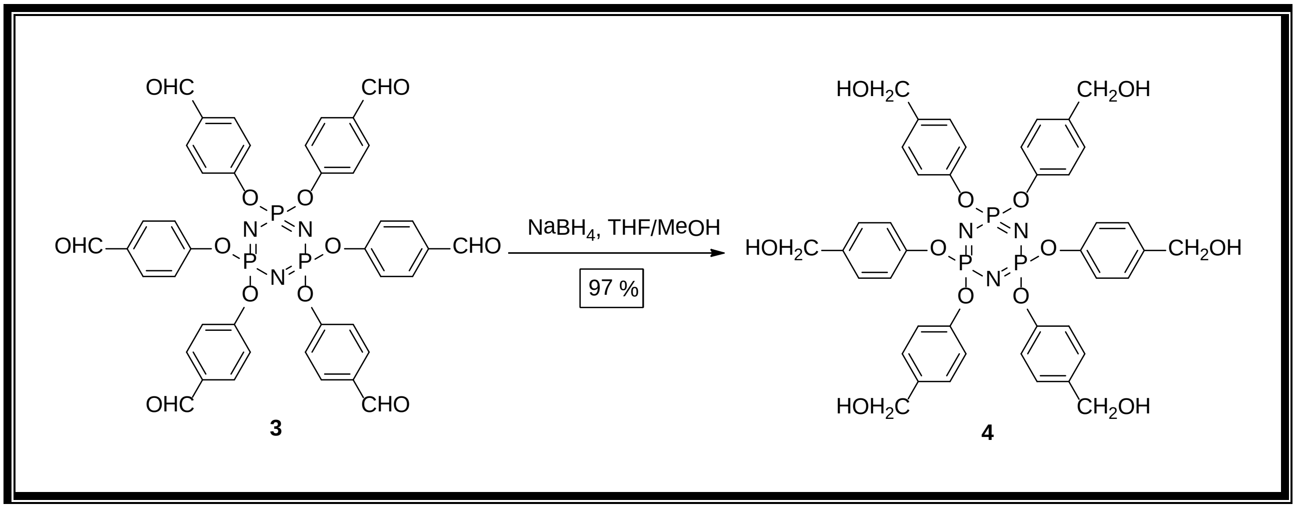

Compound **4** was prepared using the literature procedure.[2] Compound **3** (10 g, 11.6 mmol) was reduced using $NaBH_4$ (4.0 g, 0.11 mol) in 200 mL of THF/MeOH. The reaction mixture was stirred overnight at room temperature followed by removal of the solvent under reduced pressure. To this residual solid was added 200 mL H_2O, and the precipitate was filtered and crystallized from MeOH to yield **4** as white crystalline solid in 97 % isolated yield. ^{1}H NMR (600 MHz, DMSO-d_6) *δ*: 7.20 (d, *J* = 8.4 Hz, 12 H), 6.82 (d, *J* = 7.8 Hz, 12 H), 5.23 (s, 6 H), 4.48 (d, *J* = 6.6 Hz, 12 H) ppm; ^{13}C NMR (600 MHz, DMSO-d_6) *δ*: 149.1, 139.9, 128.1, 120.6, 62.7 ppm; ^{31}P NMR (600 MHz, DMSO-d_6) *δ*: 8.87 ppm.

5. Synthesis of hexakis(4-chloromethylphenoxy)cyclotriphosphazene (5)

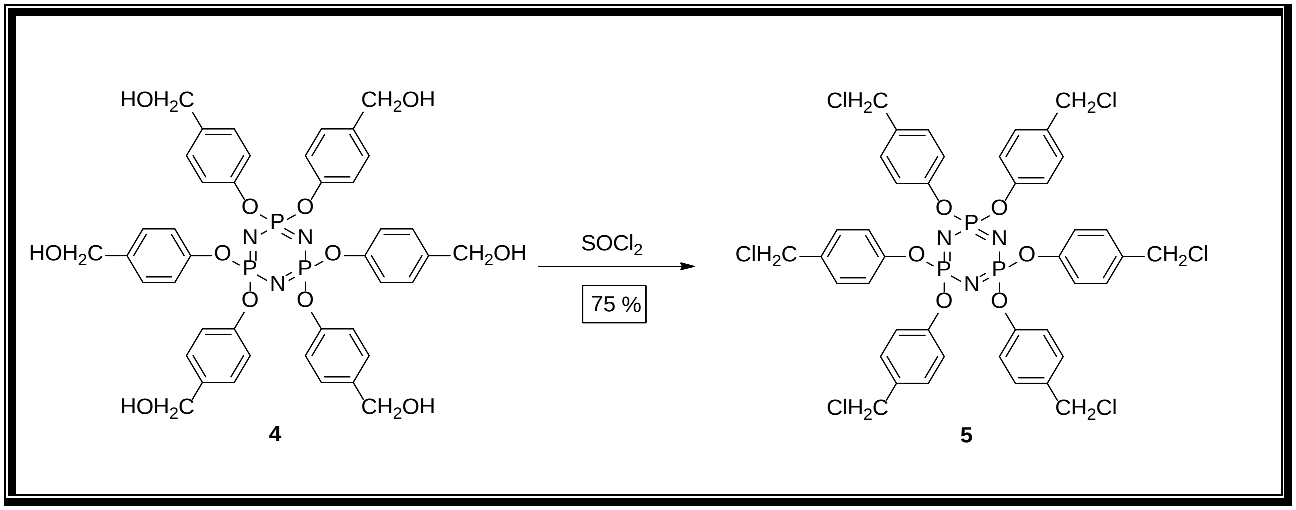

Compound **5** was prepared using the literature procedure.[2] Compound **4** (5.0 g, 5.7 mmol) was chloromethylated with thionyl chloride $SOCl_2$ (82 g, 0.69 mol). The reaction was stirred at room temperature overnight. After removing of $SOCl_2$ under reduced pressure, the crude product was recrystallized from chloroform to obtain **5** as a white crystalline compound in 75 % isolated yield. ^{1}H NMR (600 MHz, D_2O) δ: 9.01 (d, J = 6.0 Hz, 2 H), 8.96 (d, J = 6.0 Hz, 2 H), 8.45 (d, J = 6.0 Hz, 2 H), 8.42 (d, J = 6.0 Hz, 2 H), 7.46 (bs, 5 H), 5.86 (s, 2 H) 4.42 (s, 3H) ppm. ^{13}C NMR (150 MHz, D_2O) δ: 150.4, 149.7, 146.3, 145.5, 132.2, 130.1, 129.7, 129.3, 127.1, 126.7, 64.8, 48.3 ppm.

6. Synthesis of hexaviologen dendrimer (6)

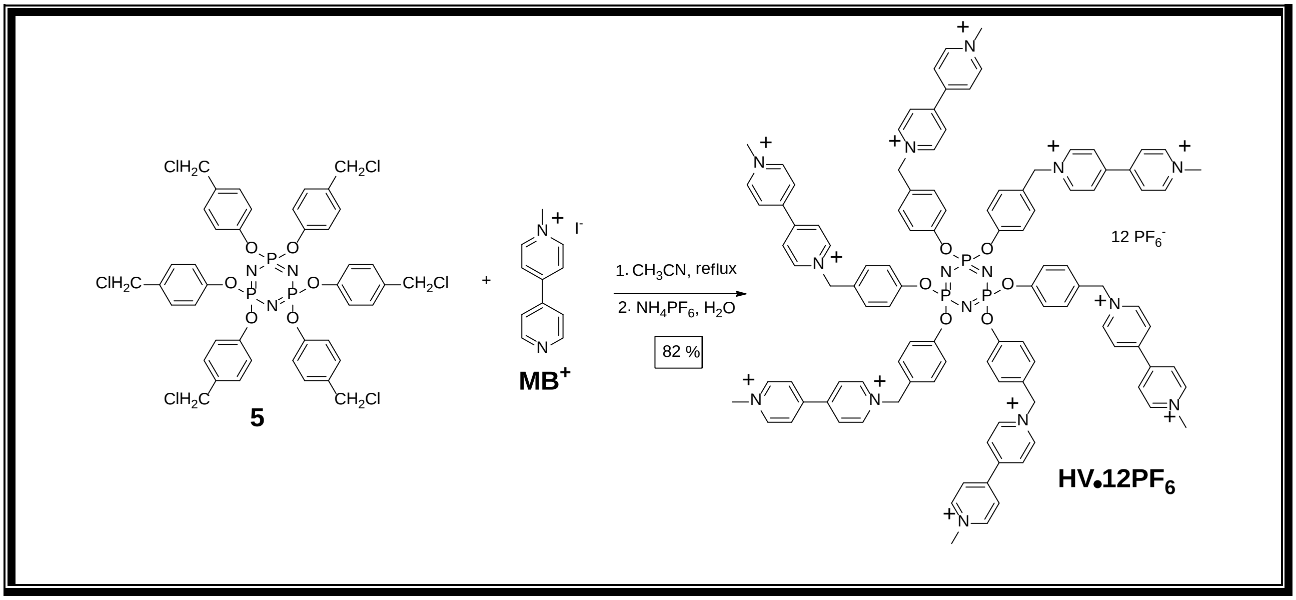

To a solution of **5** (91 mg, 0.1 mmol) in MeCN was added 298 mg (1 mmol) of 1-methyl-4,4'-bipyridinium iodide (**MB**$^+$•I). The mixture was refluxed for 48 h. The product was filtered and washed extensively with MeCN to remove unreacted **MB**$^+$. The compound obtained was dissolved in water followed by addition of ammonium hexafluorophosphate. The resulting precipitate was filtered and washed with excess water and dried under vacuum to afford 82% **HV**•12PF$_6$ as a brown solid. ^{1}H NMR (600 MHz, D$_2$O) δ: 9.15 (d, J = 12 Hz, 12 H), 9.04 (d, J = 6.0 Hz, 12 H), 8.54 (d, J = 6.0 Hz, 12 H), 8.50 (d, J = 6.0 Hz, 12 H), 7.62 (d, J = 12 Hz, 12 H),7.13 (d, J = 12 Hz, 12 H), 6.01 (s, 12H), 4.49 (s, 18 H) ppm. ^{13}C NMR (600 MHz, D$_2$O) δ: 150.51, 149.54, 146.33, 145.40, 131.79, 129.91, 127.22, 126.73, 121.98, 63.60, 49.39 ppm. ^{31}P NMR (600 MHz, D$_2$O) δ: 8.78 ppm. ESI-HRMS calcd for m/z = 1624.3172 [M – 2PF$_6$]$^{2+}$, found m/z = 1624.2183, calcd for m/z = 1034.5581 [M – 3PF$_6$]$^{3+}$, found m/z = 1034.4762, calcd for m/z = 739.6785 [M – 4PF$_6$]$^{4+}$, found m/z = 739.6170.

7. Synthesis of 1-methyl-1'-benzyl-4,4'-dipyridinium salt BMV^{2+}

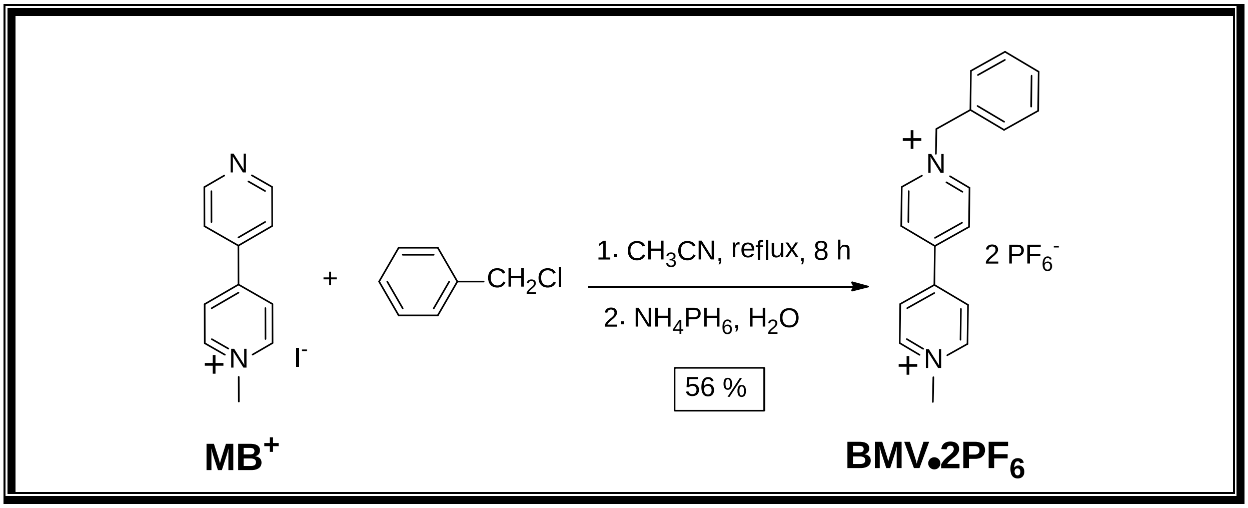

To a solution of **MB**$^{+}$ (1 mmol) in MeCN (50 mL) was added equimolar benzyl chloride. The reaction mixture was refluxed for 8 hours, followed by filtering the resulting precipitate and washing the residue with excess MeCN. The resulting precipitate was dissolved in water followed by addition of ammonium hexafluorophosphate. Precipitate obtained was filtered and washed with excess water and dried in vacuum to obtain the final product as white solid in 95% isolated yield. ^{1}H NMR (600 MHz, D_2O) δ: 9.01 (d, J = 6.0 Hz, 2 H), 8.96 (d, J = 6.0 Hz, 2 H), 8.45 (d, J = 6.0 Hz, 2 H), 8.42 (d, J = 6.0 Hz, 2 H), 7.46 (bs, 5 H), 5.86 (s, 2 H) 4.42 (s, 3H) ppm. ^{13}C NMR (150 MHz, D_2O) δ: 150.4, 149.7, 146.3, 145.5, 132.2, 130.1, 129.7, 129.3, 127.1, 126.7, 64.8, 48.3 ppm. ESI-HRMS calcd for m/z = 408.1145 $[M – PF_6]^{+}$, found m/z = 408.3087.

8. ^{1}H NMR Spectroscopic Characterization of Compound 6

The ^{1}H NMR spectra of the water soluble **HV**$^{12+}$ and **BMV**$^{2+}$ in D_2O are presented in Figure S1 and Figure S2, respectively. All the assignments have been made based on ^{1}H–^{1}H gradient-selected double-quantum filtered phase-sensitive COSY, recorded in D_2O at 298 K. The COSY spectrum of **HV**$^{2+}$ and **BMV**$^{2+}$ are shown in Figure S1b and S2b, respectively. Some of the key correlation peaks are labeled in the spectrum.

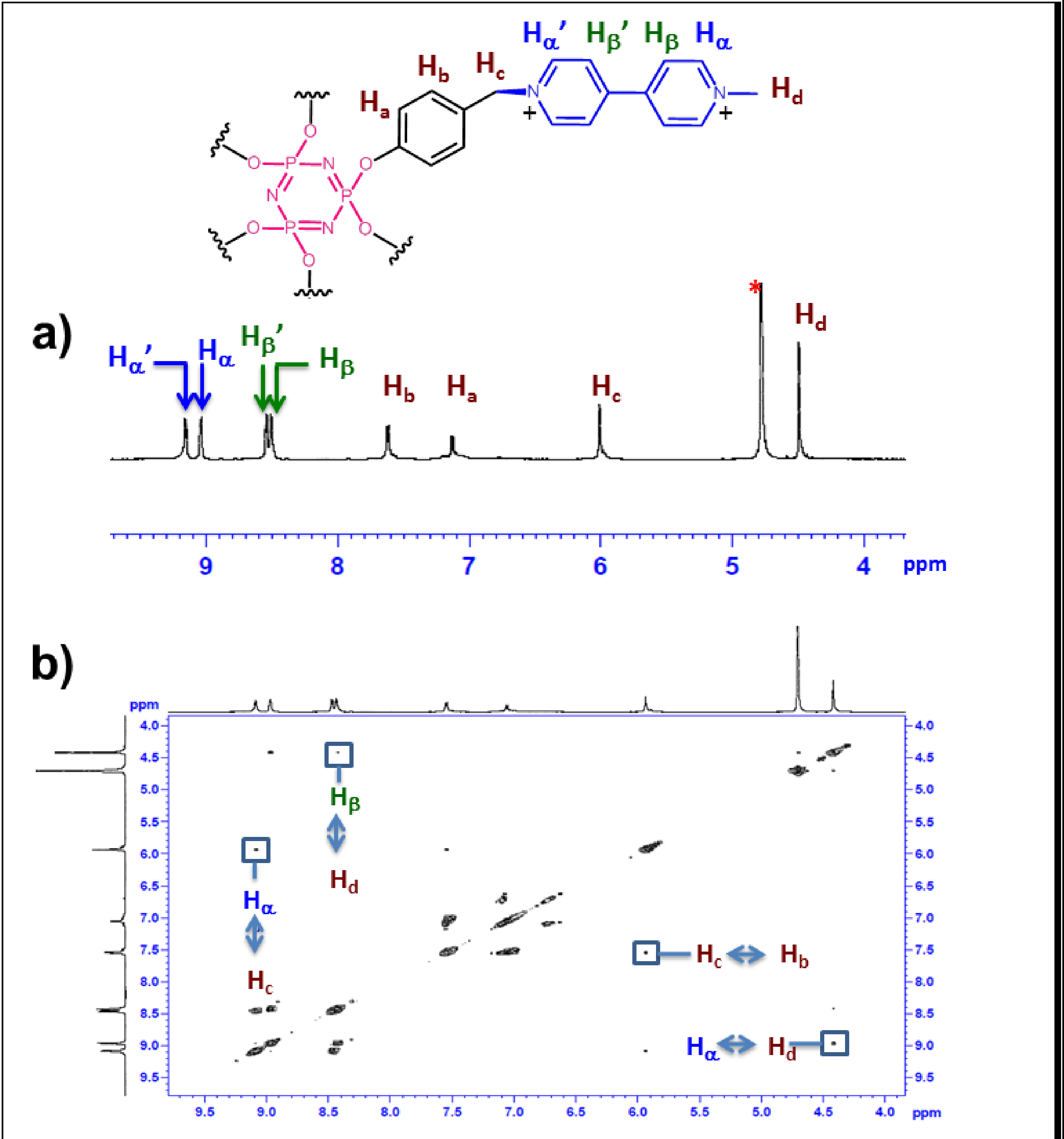

Figure S1. a) ^{1}H NMR of **HV^{12+}** in D_2O (600 MHz) and b) ^{1}H–^{1}H gradient-selected double-quantum filtered phase-sensitive COSY NMR of **HV^{12+}** in D_2O at 298 K (600 MHz). * Solvent peak.

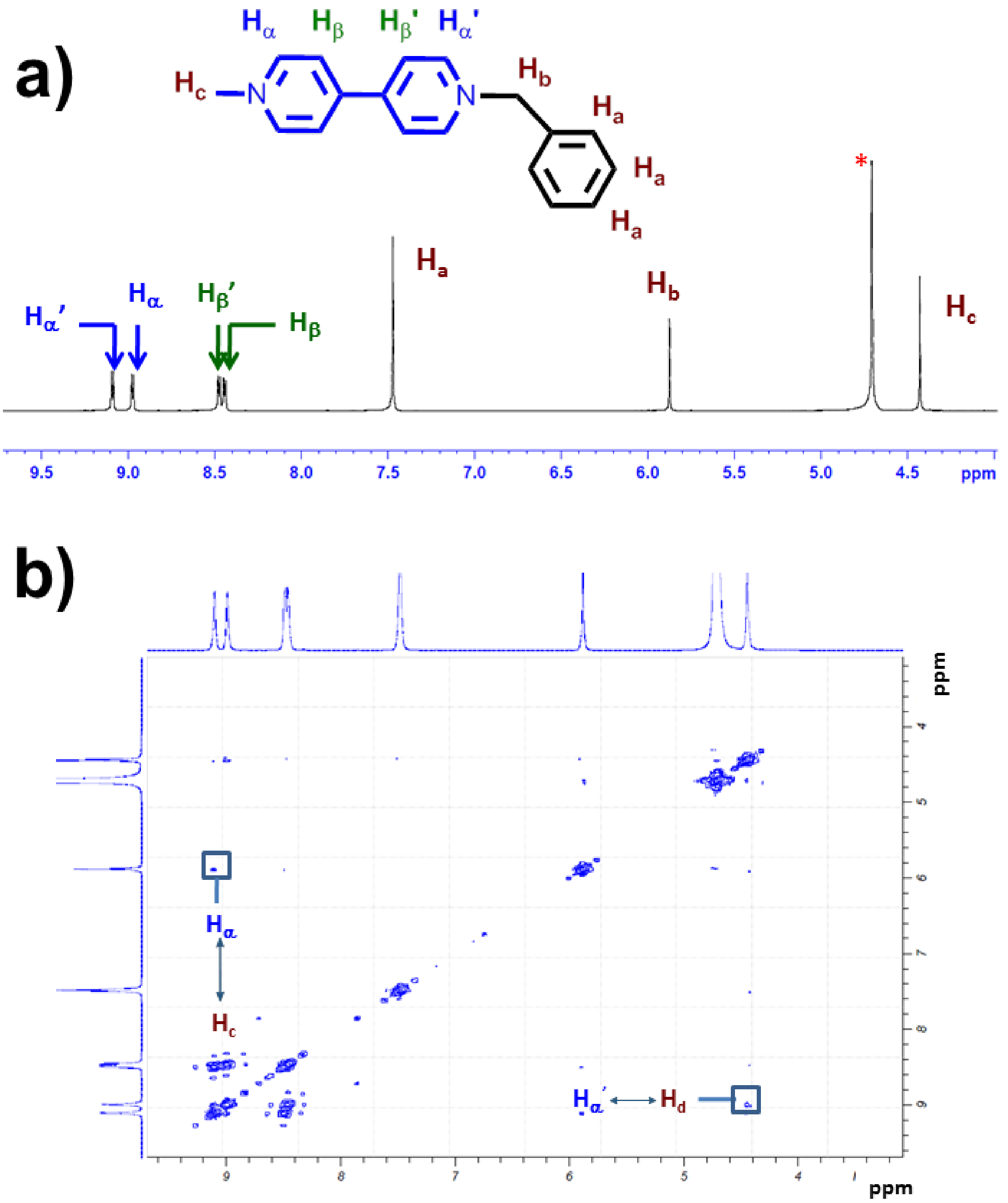

Figure S2. a) ^{1}H NMR of **BMV^{2+}** in D$_2$O (600 MHz) and b) ^{1}H–^{1}H gradient-selected double-quantum filtered phase-sensitive COSY NMR of **BMV^{2+}** in D$_2$O at 298 K (600 MHz). * Solvent Peak.

9. ^{1}H NMR DOSY

In order to measure the diffusion coefficient of **HV^{12+}** and **BMV^{2+}** in DMF for the purposes of confirming a six and a one-electron reduction takes place, respectively (see Electrochemistry Section) at a potential of approximately –0.5 V as determined by CV, an ^{1}H NMR DOSY spectrum was recorded in DMF(d7). **HV^{12+}** and **BMV^{2+}** were found to have a diffusion coefficient (*D*) equal to 1.1×10^{-6} cm^2 s^{-1}, and 4.02×10^{-6} cm^2 s^{-1} respectively.

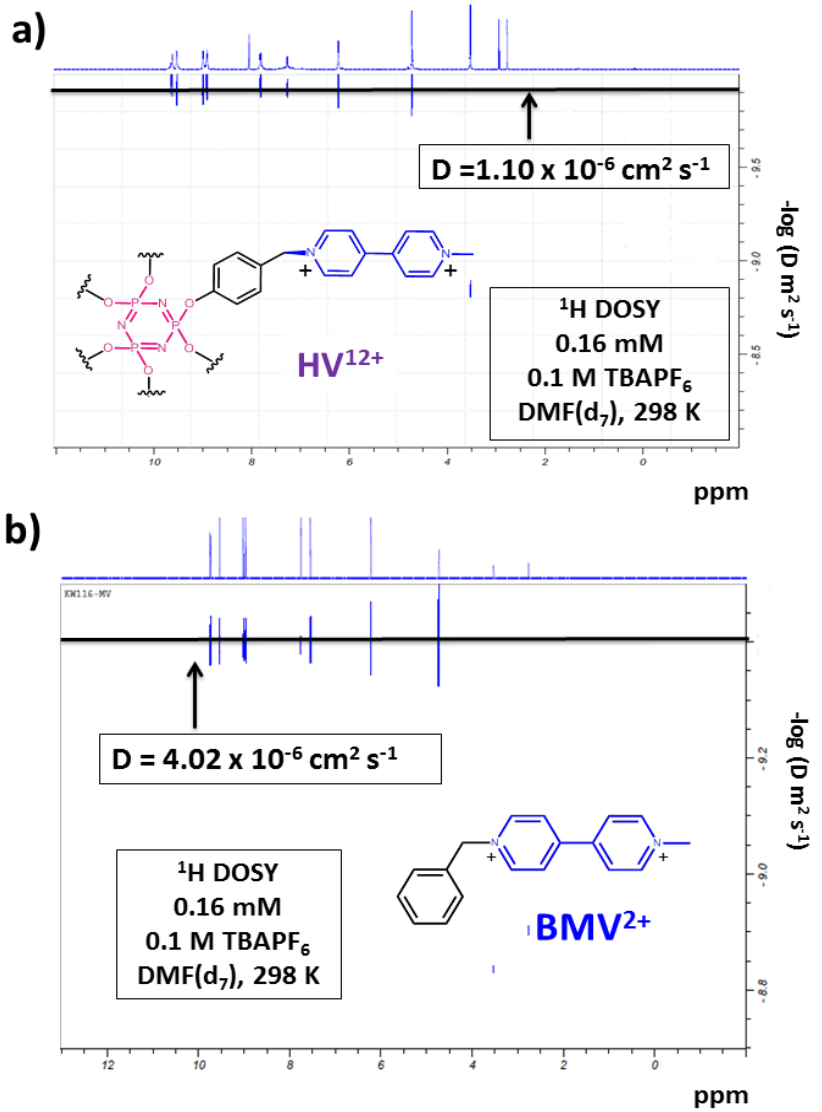

Figure S3. ^{1}H NMR DOSY spectra for a) **HV^{12+}** and b) **BMV^{2+}** in DMF(d7) containing 0.1 M of TBAPF$_6$.

10. Chrono-coulometric experiments

Chrono-coulometry experiments were performed on a 0.16 mM and 1 mM solutions of $\mathbf{HV}^{12+}$ and $\mathbf{BMV}^{2+}$ respectively in DMF (0.1 M $TBAPF_6$) in order to demonstrate that the reduction events observed in the CV in DMF at approximately –0.5 V is a six and one-electron process, respectively. The results are shown in Figure S4 as an integrated Cottrell plot. In a typical run, the potential was stepped from 0 to –0.5 V, the response was measured, and then the potential was stepped back from –0.5 to 0 V, and again the response was recorded. Making use of the Anson equation,[3] we can generate the following equality for the number of electrons transferred:

$$n = \frac{(Q/t^{1/2})\sqrt{\pi}}{2FACD^{1/2}}$$

Where n is the number of electrons transferred, $Q/t^{1/2}$, is the slope of the integrated Cottrell plot (Figure S4a, |m| = 9.33 or 8.01 μC $s^{-1/2}$ for $\mathbf{HV}^{12+}$ and |m| = 17.51 or 17.12 μC $s^{-1/2}$ for $\mathbf{MBV}^{2+}$), *F* is Faraday's constant, *A* is the area of the electrode (0.071 cm^2), *C* is the concentration of the sample, and *D* is the diffusion coefficient of either $\mathbf{HV}^{12+}$ or $\mathbf{BMV}^{2+}$ in DMF. Knowing all these parameters, we can calculate *n*, which we find to be equal to 6.9 for $\mathbf{HV}^{12+}$ and 1.0 for $\mathbf{BMV}^{2+}$. This outcome is consistent with the expected value of 6.0 for $\mathbf{HV}^{12+}$, with one electron going to each $\mathbf{BIPY}^{2+}$ unit of the $\mathbf{HV}^{12+}$.

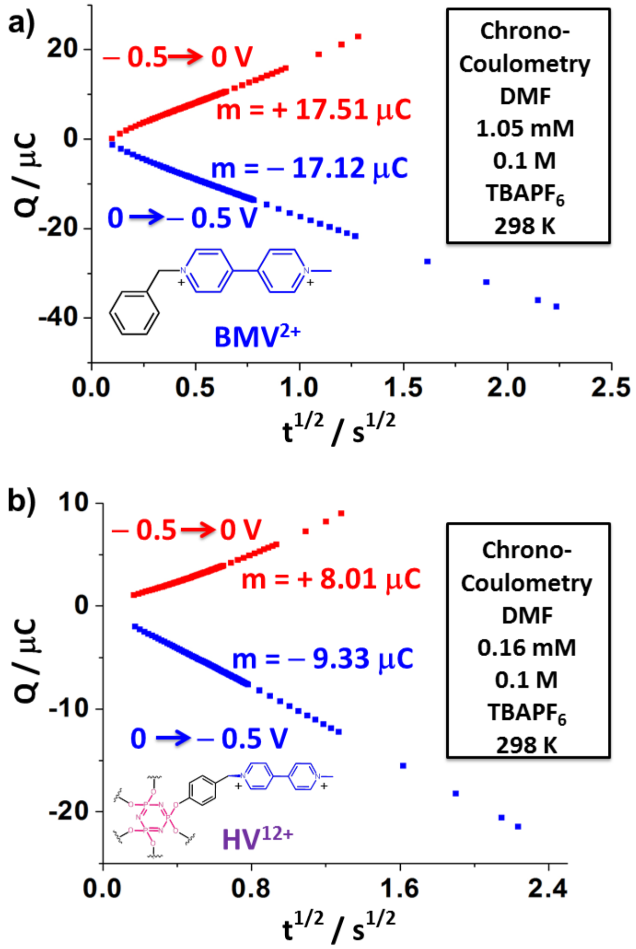

Figure S4. Integrated Cottrell chronocoulometry plots of a) **BMV**$^{2+}$ and b) **HV**$^{12+}$. The data was recorded at 298 K, in argon-purged DMF, at a concentration: [**HV**$^{12+}$] = 0.16 mM, [**BMV**$^{2+}$] = 1 mM and electrolyte: 0.1 M (TBAPF$_6$). The voltage was stepped from 0 V to –0.5 V, and the response was recorded. Application of the Anson equation using a value for the diffusion coefficient obtained from ^{1}H DOSY NMR allowed us to determine that the reduction peak for **HV**$^{12+}$ is a six-electron process.

11. UV-Vis-NIR Spectroscopy

Figure S5 shows the UV-Vis-NIR absorption spectra of **BMV**$^{2+}$ and **HV**$^{12+}$ in their ground states. The comparison of these two absorption spectra shows that in **HV^{12+}** there is no interaction between the viologens in the ground state. All spectra were recorded in MeCN at 298 K in a quartz cell with 10 mm cell path length.

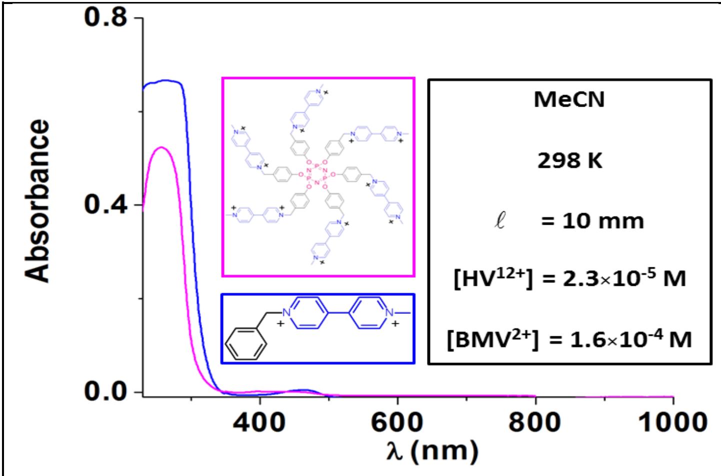

Figure S5. The outcomes of the UV-Vis-NIR carried out on **BMV^{2+}** and **HV^{12+}** in MeCN at room temperature.

Figures S6 shows the UV-Vis-NIR absorption spectra of **MV^{2+}** (a) and **HV^{12+}** (b) after being reduced with zinc dust at various concentrations in argon-purged MeCN. The reduction of both **BMV^{2+}** and **HV^{12+}** in DMF using zinc dusted resulted in what we suspect to be a complete reduction which was observed by the change of color from colorless to green after being purple for some time. For this reason MeCN was chosen as solvent for our UV/VIS/NIR measurements. While the spectrum of B**MV**$^{\bullet+}$ radical cation is consistent with its well-studied monomeric form,[4] the spectra recorded for **HV**$^{(6\bullet+)}$ at different concentrations show characteristic bands of radical-radical dimerization. Plotting the absorbance versus concentration at 600 nm for **BMV^{2+}**

and 540 nm and 870 nm for **HV^{12+}** show that in both cases absorption obey the Beer-Lambert law.

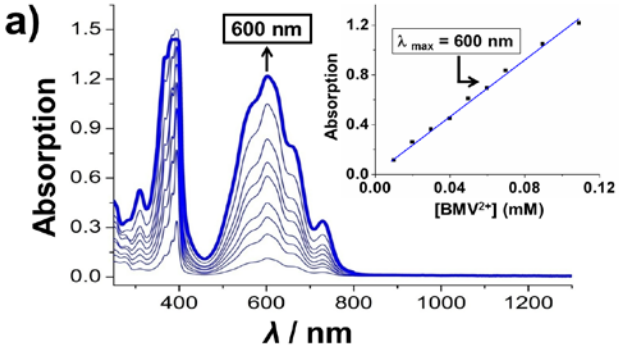

Figure S6a. The spectra UV-Vis-NIR carried out on **BMV^{2+}** at different concentration. All spectra were recorded in argon-purged acetonitrile in a 10 mm cell path length, under the same condition of temperature (298 K). At each time **BMV$^{+•}$** was generated by adding zinc dust in argon-purged acetonitrile; formation of a blue compound characterized by a set of vibronic bands centered at 400 nm and 600 nm. No evidence for dimerization or oligomerization processes (absorption > 800 nm).

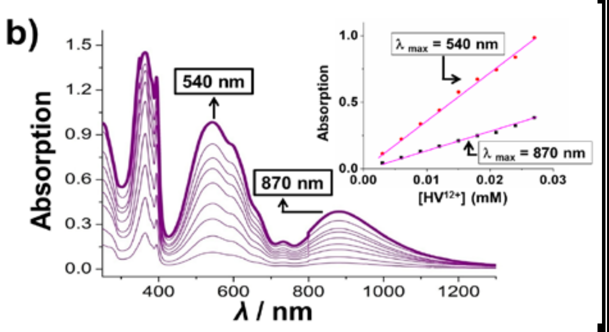

Figure S6b. The outcomes of the UV-Vis-NIR carried out on **HV^{12+}** at different concentration. All Spectra were recorded in argon-purged acetonitrile in a 10mm cell path length, under the same condition of temperature (298 K). At each time **HV$^{(6+•)}$** was generated by adding zinc dust in argon-purged acetonitrile; formation of a purple compound characterized by a set of vibronic bands centered at 370, 540 and 870 nm, respectively provide evidence for intramolecular dimerization. These data clearly demonstrate that the intramolecular dimerization processes within the **HV$^{(6+•)}$** is characterized by a high β_{Dim} dimerization constant.

12. Electrochemistry

Cyclic voltammetry (CV) experiments were performed using a glassy carbon working electrode (0.071 cm^2). The electrode surface was polished routinely with 0.05 μm alumina-water slurry on a felt surface immediately before use. The counter electrode was a Pt coil and the reference electrode was a Ag/AgCl electrode. For all measurements recorded in organic solvents (acetone, MeCN and DMF), ferrocene was added as an internal reference. In all measurements, the concentrations of the samples were 0.16 mM and 1 mM for **HV^{12+}** and **BMV^{2+}**, respectively and

0.1 M for the supporting electrolytes tetrabutylammonium hexafluorophosphate ($TBAPF_6$) in organic solvents and sodium chloride (NaCl) in H_2O. The scan rate was set to 200 mV s^{-1}.

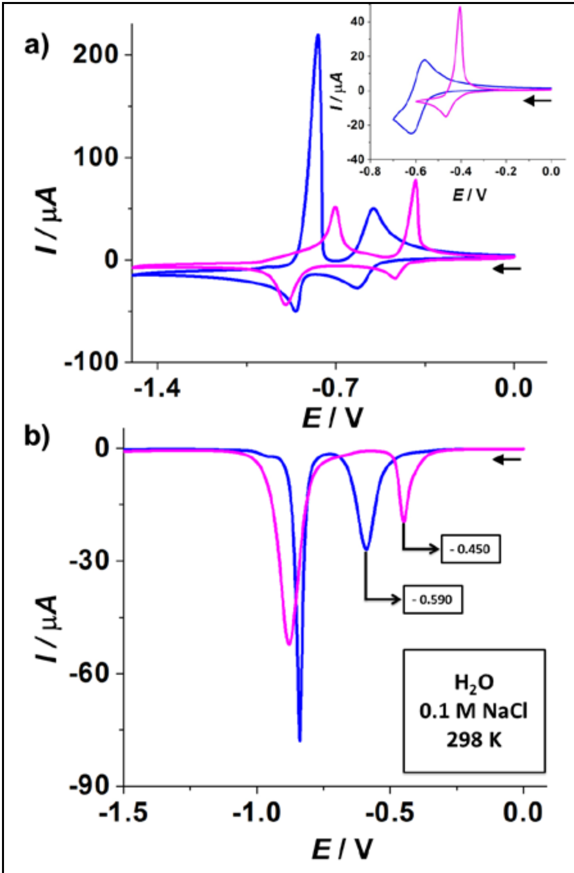

Figure S7: Second scans of the cyclic voltammograms (CVs) a) and Square-wave voltammetry b) for the $\mathbf{HV^{12+}}$ (purple traces), and $\mathbf{BMV^{2+}}$ (blue traces). All the CVs were recorded under the same conditions of temperature (298 K), solvent (argon-purged H_2O), concentrations (1 mM and 0.16 mM $\mathbf{BMV^{2+}}$ and $\mathbf{HV^{12+}}$ respectively) and electrolyte (0.1 M **NaCl**). The scan rate was set at 200 mV s^{-1}.

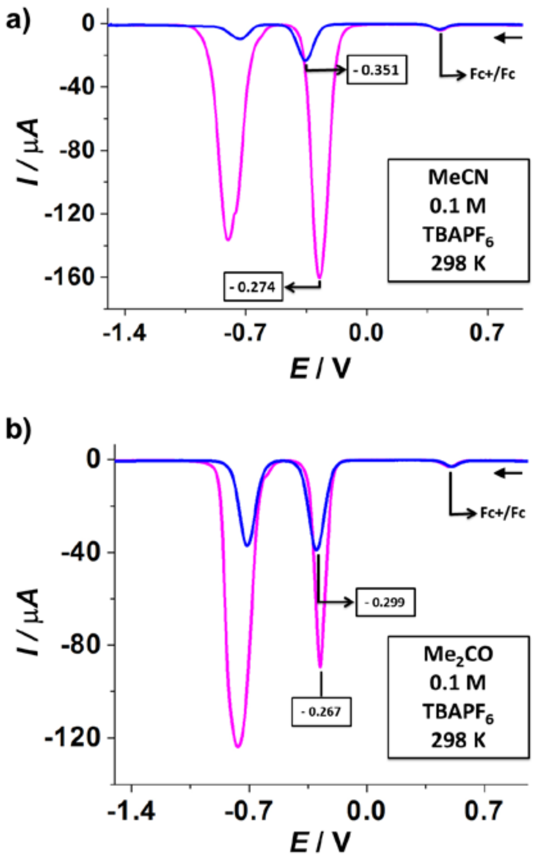

Figure S8: Square-wave voltammetry for $\mathbf{HV^{12+}}$ (purple traces), and $\mathbf{BMV^{2+}}$ (blue traces) in MeCN (1 mM for both) a) and Me_2CO (0.33 mM for $\mathbf{HV^{12+}}$ and 1 mM for $\mathbf{BMV^{2+}}$) b). Electrolyte (0.1 M $\mathbf{TBAPF_6}$).

With equation (6) in hand, we have now a means of evaluating β_{Dim}, which we have done in a variety of solvents.

$$\beta_{Dim} = \exp[(E_{eq} - E_o)/(RT/nF)] \qquad \text{Eq. (6)}$$

In each case, the global dimerization constant is high, a strong indication for efficient and almost quantitative dimerization processes (**$HV_D^{6(\bullet+)}$** represents 99.91% (Me_2CO), 99.99% DMF) and ~ 100% (MeCN and H_2O) of the overall species regardless of the concentration used). Moreover, these thermodynamic data illustrate that the dimerization processes within **$HV^{6(\bullet+)}$** are by far favored in water with respect to acetonitrile, dimethylformamide or acetone. Monomer-dimer equilibrium is indeed usually prevented in polar organic solvents, presumably because the radical cation exists as an ion pair rather than as a fully dissociated species, thus preventing the formation of the dimer.

Table S1. Thermodynamic parameters associated with the intramolecular dimerization of BIPY$^{\cdot+}$ radical cations in the dendrimer HV^{12+} after reduction in different solvents.

Solvent	E_0 / V	E_{eq} / V	ΔE / V	β_{Dim}
Me_2CO[a]	–0.299	–0.267	0.0316	1.16×10^3
DMF[a]	–0.318	–0.277	0.0404	1.26×10^4
MeCN[a]	–0.351	–0.274	0.0775	7.32×10^7
H_2O[b]	–0.593	–0.450	0.1402	1.69×10^{14}

T = 298 K. Determined from Square wave differential pulse. [a]Reference ferrocene. [b]Reference Ag/AgCl

The stability of

13. Digital Simulations

The heterogeneous electron transfer reactions (Table S1) were derived using the ladder scheme outlined in Figure S9. The experimentally determined reduction potentials for each electron transfer reaction are also given in Table S1. Heterogeneous electron transfer rate constants were assumed to be much higher than those for the homogeneous chemical reactions

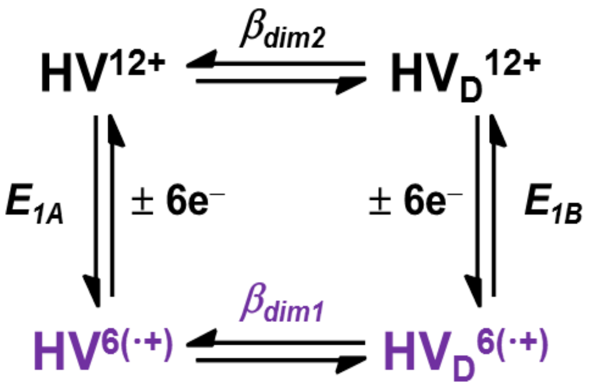

Figure S9: Square scheme mechanism for the formation of **$HV_D^{6(\bullet+)}$** (**$HV_D^{6(\bullet+)}$** stands for a hexaviologen-phosphorus dendrimer which contains three pairs of **$BIPY^{\bullet+}$** firmly stacked together).

Table S2. Heterogeneous Electron Transfer Reactions

Reaction		**E / V**
1	**$HV^{12+} + 6e^{-} = HV^{6(\cdot+)}$**	**– 0.32**
2	**$HV_D^{12+} + 6e^{-} = HV_D^{6(\cdot+)}$**	**– 0.20**

Table S3. Homogeneous Chemical Reactions

Reaction		β_{Dim}	k_f (s^{-1})	k_b (s^{-1})
3	$HV^{12+} = HV_D^{12+}$	*	*	10^8
4	$HV^{6(\cdot+)} = HV_D^{6(\cdot+)}$	**Variable**	7×10^8	*

**Calculated automatically by the program*

The homogenous chemical reactions (Table S3) were also derived using the ladder scheme in Figure S9. Inputting the reduction potentials (Table S2) into the digital simulation software produced the equilibrium constants shows in entries 3-4 listed in Table S3.

Figure S10 shows the simulated data obtained for the first reduction peak of **HV^{12+}**. These data reveals that for a change of one order of magnitude for the dimerization constant, the reduction peak change by 10 mV, which is consistent with our proposed mechanism.

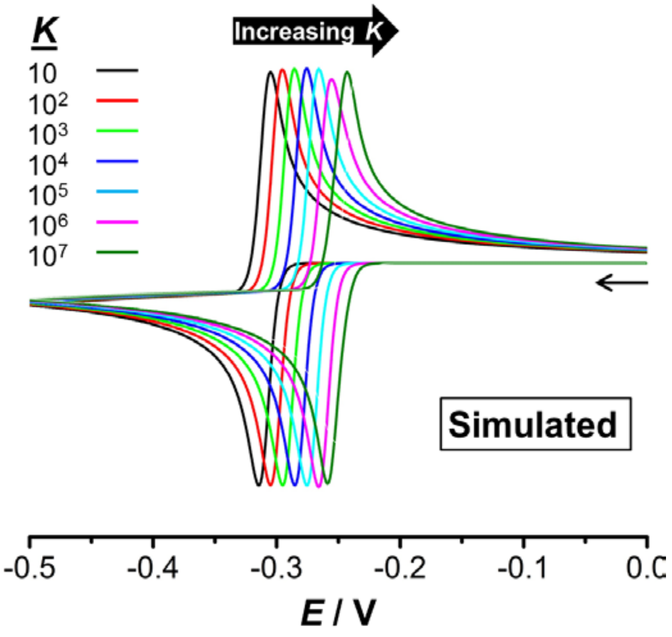

Figure S10: simulated data obtained for the first reduction peak of **HV^{12+}**.

14. Computed Molecular Geometries

In order to obtain insight into the nature of the pimerization process we have performed density functional theory calculations at the M06/6-31G(d,p) level.[5, 6] The optimized geometry of the **BV**$^{2(\bullet+)}$ system calculated in the gas phase (Figure S11) provided a molecular geometry in which the two **BIPY**$^{\bullet+}$ units are placed far away from each other.

Calculations on the **BV**$^{2(\bullet+)}$ system were performed for both the singlet and triplet states, in the latter case by using an unrestricted model. The absence of significant spin contamination was confirmed by a comparison of the expected difference between $S(S+1)$ for the assigned spin state ($S(S+1) = 2$) and the actual value of $\langle S^2 \rangle$. According to our calculations the triplet state is more stable than the singlet state by 20.6 kJ·mol^{-1}.

BV^{4+} M06/6-31G(d,p) (aqueous solution, E(RM06) = -3408.53662752 a. u.)

P	1.29737500	-1.19789000	-1.29246400
P	2.80716200	-3.06596000	0.14010700
P	0.10819400	-2.72116800	0.70843800
O	1.46994500	0.38453400	-1.12946200
O	1.08720900	-1.39702100	-2.86582000
O	3.94801600	-2.82517900	1.22155100
O	3.40207500	-4.33674600	-0.63838500
O	-1.03672400	-3.84376000	0.64137700
O	-0.34963200	-1.97815100	2.08373000
N	2.69449900	-1.82190300	-0.85940400
N	1.48374200	-3.48089500	0.93913600
N	-0.01024900	-1.71365300	-0.51627400
C	-2.32919500	-3.53620500	0.24246100
C	-2.68818600	-3.76991800	-1.07655400
C	-3.24624100	-3.07499800	1.18005500
C	-3.99972000	-3.52857300	-1.46818100
H	-1.94439600	-4.14523100	-1.77466700
C	-4.55516800	-2.84937700	0.78039100
H	-2.93116200	-2.91555500	2.20686800
C	-4.93970000	-3.07487500	-0.54383900
H	-4.29681000	-3.70830800	-2.49931700
H	-5.28595700	-2.50173500	1.50904000
C	0.49205300	-0.96443300	2.51857000
C	1.43627700	-1.25045700	3.49492400
C	0.37397500	0.30790800	1.96825900
C	2.29282800	-0.24054700	3.91702400

H	1.50002800	-2.25641800	3.89931100
C	1.23961500	1.30507500	2.39108600
H	-0.38011400	0.49256500	1.20860900
C	2.20733200	1.03608100	3.36152400
H	3.03718300	-0.45001900	4.68297200
H	1.16215200	2.30039700	1.95531200
C	-6.36426800	-2.87062900	-0.96394400
H	-7.05396700	-3.49008900	-0.38438800
H	-6.51031800	-3.10839400	-2.02183800
C	3.17874200	2.10400200	3.76654700
H	2.69231400	3.06308200	3.96154100
H	3.74705000	1.82494300	4.65826500
C	-7.87154300	-1.18643300	0.01037600
C	-6.14550800	-0.47338900	-1.40931500
C	-8.31091100	0.10959400	0.17133400
H	-8.35006500	-2.02930600	0.49678600
C	-6.54153800	0.83733000	-1.27960500
H	-5.29903600	-0.77690200	-2.01733400
C	-7.64695200	1.14892000	-0.48158700
H	-9.15644500	0.29652700	0.82465100
H	-6.00148200	1.60351100	-1.82564900
C	-8.10881300	2.54139000	-0.33694200
C	-7.19919100	3.60125800	-0.27814000
C	-9.47187900	2.82995900	-0.25961800
C	-7.66535600	4.88846200	-0.14335100
H	-6.12779100	3.43478000	-0.30956400
C	-9.88684300	4.13771400	-0.13251600
H	-10.22310800	2.05023500	-0.32478200
H	-7.00864800	5.74960800	-0.08508700
H	-10.93325500	4.41514700	-0.07982200
C	-9.43603000	6.53804700	0.05849900
H	-8.98195300	6.96964800	0.95149400
H	-9.12624900	7.09511400	-0.82720100
H	-10.52036600	6.55915200	0.14885700
N	-6.81087500	-1.45912400	-0.77216100
N	-8.98922000	5.13961200	-0.07484500
C	4.17417700	3.51947300	2.00825500
C	5.03991100	1.36814600	2.35675800
C	5.06095300	3.73875700	0.97528500
H	3.44750500	4.26179500	2.32020600
C	5.94848000	1.53836300	1.33933100
H	4.97681700	0.45556200	2.94075600
C	5.96656000	2.73789300	0.62069900
H	5.01368300	4.68201400	0.44135400
H	6.65221200	0.73993700	1.12983500
C	6.92056300	2.92543000	-0.48737700
C	7.25566300	1.85522500	-1.31809300
C	7.51210200	4.16818800	-0.73153600
C	8.15207800	2.04423000	-2.34743900
H	6.80872900	0.87428200	-1.19258300
C	8.40491500	4.30221300	-1.76960300
H	7.30760200	5.03063800	-0.10608600
H	8.44049200	1.24699600	-3.02258300
H	8.90254000	5.23785300	-2.00052800
C	9.67151400	3.44956400	-3.65825200
H	9.25619400	4.17026400	-4.36425300
H	10.60825200	3.82622900	-3.24524000

H	9.84344600	2.49796800	-4.15801700
N	4.17310000	2.35093700	2.67639500
N	8.71162300	3.25053200	-2.55716500
C	0.46477200	1.23927600	-1.67804600
H	0.60255000	1.34270500	-2.75932700
H	-0.54197400	0.85630800	-1.46963400
H	0.57930800	2.21372800	-1.20008100
C	-0.17047800	-1.69196400	-3.47890100
H	0.01460800	-2.41821400	-4.27264100
H	-0.87492500	-2.10996100	-2.75324400
H	-0.58904400	-0.77766700	-3.91116100
C	2.67677500	-4.77864100	-1.78785700
H	2.69007700	-4.01030300	-2.56923000
H	3.16948300	-5.68081400	-2.15125900
H	1.63798300	-5.01718800	-1.52323800
C	5.28364100	-2.56718600	0.77039600
H	5.85101200	-2.23589400	1.64106800
H	5.72794200	-3.47986000	0.36309300
H	5.28907000	-1.78105700	0.00735500

BV$^{2(\bullet+)}$ M06/6-31G(d,p) (triplet, aqueous solution, E(UM06) = -3408.85034161 a. u.)

P	-6.80434800	-0.76218200	-0.25915300
P	-4.37213800	-2.13719800	-0.48574300
P	-4.39986400	0.63095900	-0.32094100
O	-7.95216400	-0.82408700	-1.35681700
O	-7.68386900	-0.74842600	1.08354500
O	-3.89680400	-2.91563200	-1.79916700
O	-3.75876600	-3.00585000	0.71315700
O	-3.96750900	1.33509800	1.07715700
O	-3.94474900	1.71564200	-1.42314200
N	-5.96645200	-2.11333900	-0.36927200
N	-3.61291700	-0.73433300	-0.53896300
N	-5.98343500	0.61434500	-0.35797100
C	-2.71853100	1.19795000	1.66369000
C	-1.91959500	2.32732100	1.76778500
C	-2.30967800	-0.03080600	2.17333600
C	-0.65630100	2.20897600	2.33341400
H	-2.27318100	3.27308000	1.36600500
C	-1.04700700	-0.13303300	2.73700600
H	-2.96474300	-0.89500400	2.10024600
C	-0.20348000	0.97849700	2.80427500
H	-0.00802100	3.08176100	2.39355700
H	-0.69961700	-1.09419700	3.11284500
C	-2.68785000	2.30520400	-1.43679600
C	-2.64375100	3.69305300	-1.39701500
C	-1.52628300	1.54894100	-1.53546100
C	-1.41230100	4.33131500	-1.44068900
H	-3.57141200	4.25352600	-1.32154800
C	-0.29944400	2.20400700	-1.58507000
H	-1.58650300	0.46437200	-1.56430000
C	-0.22988400	3.59563600	-1.53866800
H	-1.36852600	5.41813500	-1.40283800

H	0.61087900	1.61160800	-1.67238700
C	1.20174600	0.82562800	3.29878200
H	1.23192700	0.34509300	4.28258200
H	1.68864000	1.80537100	3.39110400
C	1.07194500	4.34284900	-1.67829400
H	1.23712500	4.63434100	-2.72218500
H	1.04126600	5.27318300	-1.09951600
C	3.00777800	-0.80450600	2.90379000
C	1.85228600	0.04478900	1.03879700
C	3.84754600	-1.50842800	2.09695700
H	3.08509600	-0.83173700	3.98575600
C	2.66717800	-0.64040500	0.19083400
H	1.03281300	0.66571900	0.68581300
C	3.74194000	-1.44232600	0.67553000
H	4.60612300	-2.11310600	2.58223800
H	2.46950900	-0.54017300	-0.87157900
C	4.66224500	-2.09342800	-0.19589700
C	4.57177100	-1.99625000	-1.61671100
C	5.76186500	-2.86402200	0.28590500
C	5.48689900	-2.59281100	-2.42838600
H	3.77492100	-1.43954900	-2.09798600
C	6.65076600	-3.44257600	-0.56804500
H	5.93135500	-3.00655200	1.34809300
H	5.43745200	-2.52378100	-3.51004600
H	7.49473800	-4.03001600	-0.22089000
C	7.55145000	-3.86179300	-2.81043200
H	7.10189600	-4.10700800	-3.77399700
H	8.35341800	-3.13192900	-2.96026900
H	7.96727600	-4.77083600	-2.37250900
N	2.01299800	-0.01799700	2.39476800
N	6.52818900	-3.31841300	-1.92318800
C	3.04318200	2.94961300	-2.16747600
C	2.54292200	3.46816000	0.07737300
C	4.13990300	2.24001200	-1.78588500
H	2.74673700	3.05154800	-3.20680400
C	3.62953800	2.77193300	0.50672800
H	1.86436700	3.97570200	0.75677000
C	4.50874800	2.12176600	-0.41250500
H	4.71510800	1.76078100	-2.57025100
H	3.80699000	2.74347700	1.57695700
C	5.65963200	1.39323700	0.00816400
C	5.97303400	1.18428100	1.38323400
C	6.57126900	0.80026800	-0.91338300
C	7.04900100	0.43955000	1.75944600
H	5.34592700	1.58243800	2.17393500
C	7.63756400	0.06760200	-0.48614000
H	6.44531100	0.90712600	-1.98513600
H	7.29412300	0.25222500	2.80012200
H	8.33758200	-0.39365900	-1.17576800
C	9.02332000	-0.92245000	1.29199500
H	9.44639200	-1.46182100	0.44329100
H	9.78908800	-0.27354600	1.72605700
H	8.69183800	-1.64537100	2.04232900
N	2.24590700	3.58300400	-1.25433600
N	7.88352300	-0.12946700	0.84020700
C	-8.89264000	0.25362400	-1.44599400
H	-9.51541400	0.29142100	-0.54735200

H	-8.37217600	1.20746300	-1.57878100
H	-9.51543600	0.05194000	-2.31764600
C	-6.98987300	-0.51772600	2.31038300
H	-7.70847300	-0.66344900	3.11726900
H	-6.16275500	-1.23057100	2.43511200
H	-6.59572700	0.50363200	2.34297100
C	-4.52923600	-3.87092100	1.55239000
H	-4.42574000	-4.90508500	1.20978000
H	-4.12956100	-3.78097600	2.56461000
H	-5.58614400	-3.58879000	1.54488900
C	-4.22614400	-4.30230000	-1.92017000
H	-4.01103400	-4.59071900	-2.94946700
H	-3.61210100	-4.90004000	-1.23824400
H	-5.28905000	-4.47284400	-1.71263000

BV$^{2(\bullet+)}$ M06/6-31G(d,p) (singlet, aqueous solution, E(RM06) = -3408.84247948 a. u.)

P	-6.61920000	-0.80247500	0.14077100
P	-4.28110000	-2.18857800	-0.54805800
P	-4.24275100	0.57293500	-0.28998700
O	-7.90167500	-0.86788400	-0.79741900
O	-7.31724600	-0.77275500	1.58433000
O	-4.12098900	-2.88507200	-1.97840300
O	-3.44316100	-3.16671300	0.40717100
O	-3.57494000	1.23288400	1.03334300
O	-3.97269100	1.69872200	-1.41116300
N	-5.80410000	-2.15759400	-0.06435200
N	-3.51828400	-0.78955400	-0.67782300
N	-5.81250200	0.56808500	-0.07472900
C	-2.30453600	0.98673400	1.52512200
C	-1.44104300	2.06769100	1.64365800
C	-1.93397300	-0.28484000	1.95240900
C	-0.17390700	1.86525300	2.17702400
H	-1.76490300	3.04861000	1.30351600
C	-0.66132900	-0.47345300	2.47101600
H	-2.62792800	-1.11555300	1.86120900
C	0.23093100	0.59426000	2.58494000
H	0.51200800	2.70564000	2.27027600
H	-0.35332800	-1.46764200	2.79137300
C	-2.74849700	2.32269800	-1.59612900
C	-2.74664100	3.71020300	-1.60004700
C	-1.58257900	1.59562200	-1.81735300
C	-1.55403300	4.38415500	-1.83296000
H	-3.67541900	4.24357000	-1.41871200
C	-0.39661700	2.28395100	-2.03623400
H	-1.61135200	0.50918100	-1.80968300
C	-0.37323000	3.68010100	-2.06178900
H	-1.54299900	5.47218900	-1.83847000
H	0.52134700	1.71988400	-2.20201000
C	1.62700800	0.35491600	3.07727900
H	1.63040700	-0.25806300	3.98441000
H	2.12541300	1.30187600	3.31907800
C	0.89850300	4.42683900	-2.36712100
H	1.14842700	4.36920600	-3.43225300
H	0.78991700	5.48930000	-2.12034700

C	3.30026600	-1.36895300	2.46407400
C	2.37264000	-0.03992000	0.75599800
C	4.12614400	-1.98313000	1.57676000
H	3.28798000	-1.62270800	3.51935700
C	3.16573900	-0.64514000	-0.17423400
H	1.63139900	0.70704400	0.48307400
C	4.13417500	-1.61124900	0.19450100
H	4.77276400	-2.76499900	1.96091800
H	3.04122600	-0.32522100	-1.20445600
C	5.03753800	-2.18976100	-0.75599900
C	5.02684300	-1.83893900	-2.13559100
C	5.99201400	-3.18152100	-0.39449700
C	5.89334400	-2.40875300	-3.01876900
H	4.32812100	-1.11019700	-2.53228400
C	6.84004300	-3.71918000	-1.31733900
H	6.07881400	-3.54066100	0.62500100
H	5.90227700	-2.15155200	-4.07289600
H	7.57787700	-4.47065900	-1.05716500
C	7.75633600	-3.88662000	-3.59131400
H	7.24617700	-4.07590700	-4.53775400
H	8.57379700	-3.17844300	-3.75329200
H	8.16000900	-4.82567000	-3.21140900
N	2.44486300	-0.37049600	2.07782100
N	6.80276600	-3.34506500	-2.62533400
C	2.99818300	3.13048200	-2.24022000
C	2.08431400	4.03348300	-0.26834700
C	3.96512100	2.48869200	-1.53051000
H	2.93491300	3.07111100	-3.32212400
C	3.03311600	3.41807500	0.48485900
H	1.31220700	4.66481500	0.16279700
C	4.00806300	2.55336300	-0.10439800
H	4.68856400	1.90934400	-2.09449600
H	3.00767700	3.59523900	1.55483600
C	4.94496900	1.81821500	0.67773900
C	4.97914800	1.89977200	2.11008000
C	5.90125900	0.93451800	0.10620900
C	5.76181700	1.06979200	2.84222400
H	4.38117900	2.62427000	2.65263200
C	6.65755400	0.10816600	0.88666900
H	6.03541400	0.85409800	-0.96818100
H	5.79105200	1.09272700	3.92678800
H	7.36862200	-0.59627000	0.46522100
C	7.35376900	-0.77816600	3.07142900
H	7.66580400	-1.63864400	2.47688800
H	8.23993400	-0.26024400	3.45196600
H	6.75262400	-1.13216800	3.91227800
N	2.04203300	3.88960900	-1.62687100
N	6.54835700	0.11528100	2.24460300
C	-8.82585100	0.22734800	-0.79136100
H	-9.32446500	0.30122100	0.17974200
H	-8.30862700	1.16577700	-1.01544600
H	-9.56183400	0.02057200	-1.56862400
C	-6.48651500	-0.48550900	2.71021800
H	-7.11501700	-0.55606200	3.59822200
H	-5.66966300	-1.21470900	2.79010500
H	-6.06529200	0.52260800	2.63219700
C	-4.03605900	-3.86026700	1.50739300

H	-4.81698900	-4.54796200	1.16807400
H	-3.23257600	-4.42545500	1.98167000
H	-4.46439900	-3.16054400	2.23284400
C	-4.56823200	-4.23688000	-2.12415200
H	-4.50488900	-4.47826500	-3.18541700
H	-3.92515000	-4.91601400	-1.55452900
H	-5.60645900	-4.34051300	-1.78930000

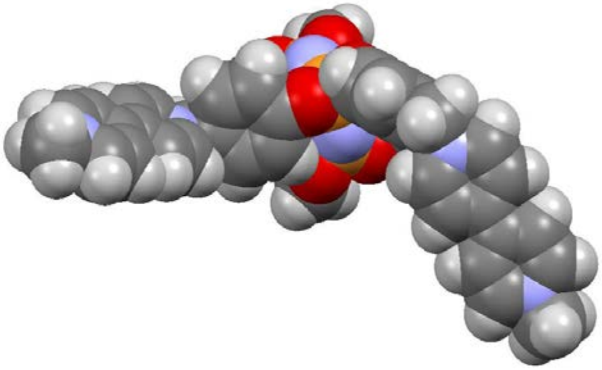

Figure S11: Optimized geometry of the **BV**$^{2(\bullet+)}$ system calculated in the gas phase provided a molecular geometry in which the two **BIPY**$^{\bullet+}$ units are placed far away from each other, unlike the geometry optimized in aqueous solution presented in the main text.

15. Stability and Reversibility of the Device

In order to obtain insight into the reversibility and the stability of the ITO-based window, we have performed 10 cycles of redox that show that no significant changes can be observed in the performance of the device (Figure S12).

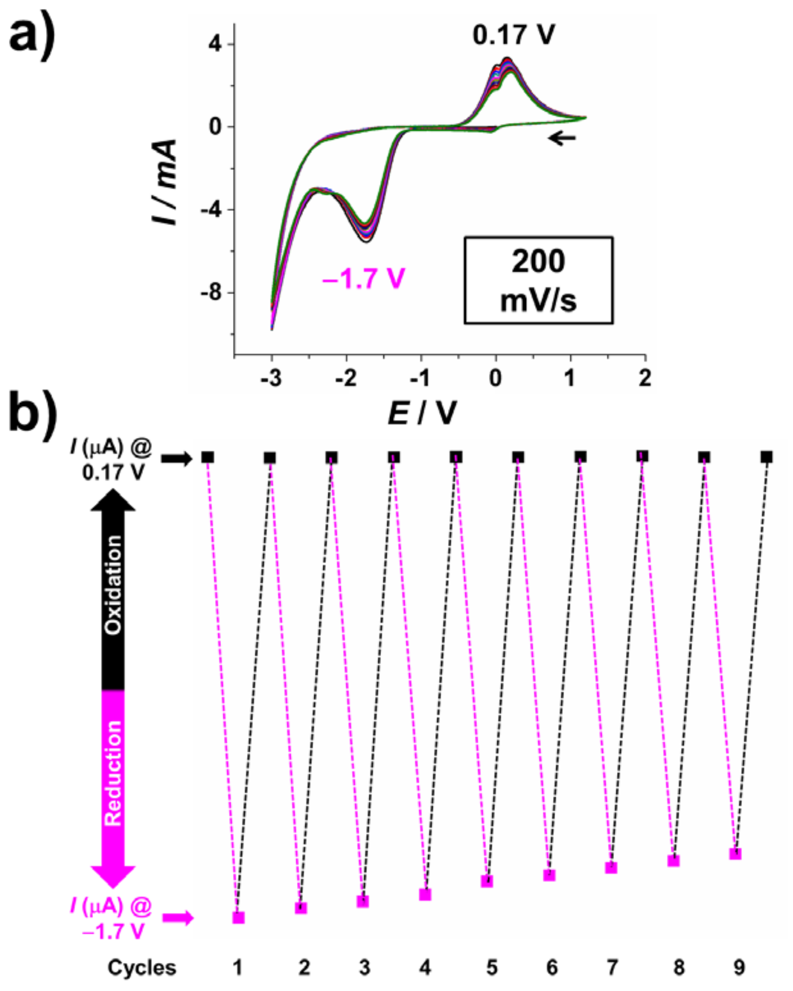

Figure S12: a) Reversible Redox cycles of the ITO device and b) change in the current intensity as a fuction of reduction/oxidation processes.

Supplementary References

[1] C. R Smith, *Synlett* **2009**, 1522–1523.

K. Inoue, S. Negayama, T. Itaya, M. Sugiyama, *Macromol. Rapid. Commun*. **1997**, *18*, 225–231.

[2] D. Quan, R. K. Nagarale, W. Shin, *Electroanalysis* **2010**, *22*, 2389–2398.

[3] A. J. Bard; L. R. Faulkner, Electrochemical Methods: *Fundamentals and Applications*, John Wiley and Sons, New York, **2001**.

[4] A. Trabolsi, N. Khashab, A. C. Fahrenbach, D. C. Friedman, M. T. Colvin, K. K. Cotí, D. Benitez, E. Tkatchouk, J. -C. Olsen, M. E. Belowich, R. Carmielli, H. A. Khatib, W. A. Goddard III, M. R. Wasielewski, J. F. Stoddart, *Nature Chem*. **2010**, *2*, 42–49.

[5] Y. Zhao, D. G. Truhlar, *Theor. Chem. Acc.* **2008**, *120*, 215–241.

[6] Gaussian 09, Revision B.1, M. J. Frisch, G. W. Trucks, H. B. Schlegel, G. E. Scuseria, M. A. Robb, J. R. Cheeseman, G. Scalmani, V. Barone, B. Mennucci, G. A. Petersson, H. Nakatsuji, M. Caricato, X. Li, H. P. Hratchian, A. F. Izmaylov, J. Bloino, G. Zheng, J. L. Sonnenberg, M. Hada, M. Ehara, K. Toyota, R. Fukuda, J. Hasegawa, M. Ishida, T. Nakajima, Y. Honda, O. Kitao, H. Nakai, T. Vreven, J. A. Montgomery, Jr., J. E. Peralta, F. Ogliaro, M. Bearpark, J. J. Heyd, E. Brothers, K. N. Kudin, V. N. Staroverov, R. Kobayashi, J. Normand, K. Raghavachari, A. Rendell, J. C. Burant, S. S. Iyengar, J. Tomasi, M. Cossi, N. Rega, J. M. Millam, M. Klene, J. E. Knox, J. B. Cross, V. Bakken, C. Adamo, J. Jaramillo, R. Gomperts, R. E. Stratmann, O. Yazyev, A. J. Austin, R. Cammi, C. Pomelli, J. W. Ochterski, R. L. Martin, K. Morokuma, V. G. Zakrzewski, G. A. Voth, P. Salvador, J. J. Dannenberg, S. Dapprich, A. D. Daniels, Ö. Farkas, J. B. Foresman, J. V. Ortiz, J. Cioslowski, and D. J. Fox, Gaussian, Inc., Wallingford CT, **2009**.